Mambin, a Potent Glycoprotein IIb–IIIa Antagonist and Platelet Aggregation Inhibitor Structurally Related to the Short Neurotoxins

Robert S. McDowell,[‡] Mark S. Dennis,[§] Andrea Louie,[∥] Michael Shuster,[⊥] Michael G. Mulkerrin,[§] and Robert A. Lazarus*,[§]

Departments of Bioorganic Chemistry, Protein Engineering, and Protein Chemistry, Genentech, Inc., 460 Point San Bruno Boulevard, South San Francisco, California 94080, and Department of Biophysics and Biochemistry, University of California, San Francisco, California 94143

Received August 20, 1991; Revised Manuscript Received February 6, 1992

ABSTRACT: The purification, complete amino acid sequence, functional activity, and structural modeling are described for mambin, a platelet glycoprotein GP IIb–IIIa antagonist and potent inhibitor of platelet aggregation from the venom of the *Elapidae* snake *Dendroaspis jamesonii* (Jameson's mamba). Mambin is 59 residues in length and contains four disulfide linkages and an RGD amino acid sequence found in protein ligands that bind to GP IIb–IIIa. Mambin inhibits ADP-induced platelet aggregation (IC_{50} = 172 ± 22 nM) and inhibits the binding of purified platelet fibrinogen receptor GP IIb–IIIa to immobilized fibrinogen (IC_{50} = 3.1 ± 0.8 nM). Mambin has very little sequence similarity to the *Viperidae* family of platelet aggregation inhibitors, except for the RGD-containing region in the protein. However, mambin does have ca. 47% similarity to the short-chain postsynaptic neurotoxins found in other *Elapidae* venoms, which do not contain the RGD sequence and do not act as GP IIb–IIIa antagonists. On the basis of its circular dichroism spectrum, mambin has a β-sheet structure characteristic of the neurotoxins. Molecular modeling of the mambin sequence onto the erabutoxin *b* structure predicts a very similar structure within the entire protein except for the loop containing the RGD sequence. Mambin may therefore represent a genetic hybrid of neurotoxic and hemotoxic proteins found in snake venoms.

The integrin family of cytoadhesive receptors and their respective ligands that mediate cell–cell and cell–matrix interactions plays a key role in cell biology (Albelda & Buck, 1990). Glycoprotein IIb–IIIa (GP IIb–IIIa)[1] is the most abundant integrin receptor on platelets and is primarily responsible for mediating platelet aggregation via its interaction with fibrinogen (Fg) (Kieffer & Phillips, 1990; Phillips et al., 1988; Plow & Ginsburg, 1989). In various in vivo models, both a monoclonal antibody to GP IIb–IIIa and kistrin, a 68-residue GP IIb–IIIa protein antagonist from the venom of *Agkistrodon rhodostoma* (Dennis et al., 1990), have demonstrated marked antithrombotic effects as well as increased thrombolysis and prevention of reocclusion when used in conjunction with tissue-type plasminogen activator (Coller et al., 1986; Gold et al., 1988; Yasuda et al., 1991). An understanding of the role of GP IIb–IIIa or other integrin receptors in normal hemostasis (Hawiger, 1990; Kieffer & Phillips, 1990) may therefore lead to new antiplatelet agents for thrombotic disease (Becker & Gore, 1991).

Snake venoms contain a complex array of biologically potent proteins that are known to affect vital functions in various ways including severe neuromuscular impairment, both promotion and inhibition of blood coagulation or platelet aggregation, tumor metastasis, cytotoxicity, and cardiovascular failure (Lee, 1979; Stocker, 1990). The structural and functional relationships of these proteins are of great interest; in particular, studies with the neurotoxins present in most *Elapidae* snakes have provided a great deal of insight into neurobiology and specifically into the structure and function of the nicotinic acetylcholine receptor (nAChR) on the postsynaptic membrane (Changeux et al., 1984; Stroud et al., 1990).

Recently, proteins from a variety of *Viperidae* snake venoms have been reported to potently inhibit platelet aggregation via antagonism of fibrinogen binding to GP IIb–IIIa (Dennis et al., 1990; Gould et al., 1990). These cysteine-rich proteins are highly homologous, and all contain the Arg-Gly-Asp (RGD) sequence, an adhesion site recognition sequence (Ruoslahti & Pierschbacher, 1987) common to adhesive protein ligands that bind to GP IIb–IIIa (Plow & Ginsburg, 1989). Furthermore, short, cysteine-rich, RGD-containing, potent protein inhibitors of platelet aggregation that are similar to those from the *Viperidae* family have been discovered in various leeches (Seymour et al., 1990; Mazur et al., 1991). The most striking features of all of these proteins are the presence of the RGD sequence and their apparent similarity in potency as platelet aggregation inhibitors.

In this report we describe a new GP IIb–IIIa antagonist and platelet aggregation inhibitor from the venom of the *Elapidae* snake *Dendroaspis jamesonii* (Jameson's mamba), which we have named mambin. Most interestingly, mambin, which bears little sequence similarity to any of the other GP IIb–IIIa antagonists previously described, shows a striking resemblance to the short-chain postsynaptic neurotoxins found in other *Elapidae* venoms such as erabutoxin *b*.

Materials and Methods

Materials. Lyophilized *D. jamesonii* snake venom was purchased from Sigma (St. Louis, MO). Endoproteinase Lys-C was purchased from Boehringer Mannheim (Indianapolis, IN). Erabutoxin *b* was obtained from Ventoxin Laboratories, Inc. (Frederick, MD). All other reagents were reagent grade or were prepared as described previously (Dennis

* To whom correspondence should be addressed.
[‡] Department of Bioorganic Chemistry, Genentech, Inc.
[§] Department of Protein Engineering, Genentech, Inc.
[∥] Department of Protein Chemistry, Genentech, Inc.
[⊥] Department of Biophysics and Biochemistry, University of California.

[1] Abbreviations: GP, glycoprotein; Fg, fibrinogen; RGD, Arg-Gly-Asp; nAChR, nicotinic acetylcholine receptor; Btx, bungarotoxin; TFA, trifluoroacetic acid.

0006-2960/92/0431-4766$03.00/0 © 1992 American Chemical Society

et al., 1990). ^{125}I-α-Bungarotoxin (Btx) at 260 Ci/mmol was purchased from Amersham. nAChR from *Torpedo californica* was purified as previously described (McCarthy & Stroud, 1989).

The peptide cyclo-CFTPRGDMPGPYC (cyclo-C43–C54) was prepared by automated solid-phase methodology on an ABI 430A synthesizer using standard *t*-Boc chemistry (Barany & Merrifield, 1980). Crude peptide was cleaved from the resin using anhydrous HF, cyclized using $K_3Fe(CN)_6$, and purified on a reverse-phase C18 column using a 0.1% TFA/acetonitrile gradient; amino acid analysis and mass spectral analysis confirmed the composition.

Purification of Mambin. Mambin was purified from lyophilized venom (5 mg in 1 mL of H_2O) by HPLC using a 5-μm, 250 × 4.6 mm Vydac C18 column (218TP-54) with a 0.1% TFA/acetonitrile gradient at 1.0% per minute from 10% to 40% acetonitrile/0.1% TFA and monitored at A_{214}. The active peak as measured by the Fg/GP IIb–IIIa ELISA was pooled and rechromatographed as above at 0.5% per minute.

Amino Acid and Sequence Analysis. Amino acid analysis, sequence analysis of native mambin (0.5 nmol), and reduction and carboxymethylation of native mambin (0.9 nmol) were carried out using methods described previously (Dennis et al., 1990). The reduced and carboxymethylated mambin was digested with 0.5 μg of endoproteinase Lys-C (Boehringer) in 100 μL of 10 mM Tris-HCl, pH 8.5, overnight at 37 °C. For cyanogen bromide (CNBr) digests, 1 nmol of reduced and carboxymethylated mambin was solubilized in 100 μL of 80% formic acid containing 0.1 mg of CNBr in the dark for 20 h at 25 °C; the sample was lyophilized and resolubilized in 6 M guanidine hydrochloride prior to HPLC purification of the peptides. Lys-C and CNBr digests were chromatographed on a Vydac C18 column as described above, and isolated peptides were sequenced.

Electrospray Ionization Mass Spectrometry. Native mambin (ca. 50 pmol) was lyophilized, redissolved in 20 μL of formic acid/acetonitrile/water (1/1/2), and infused toward the mass spectrometer at 5 μL/min flow. A Sciex API3 biomolecular mass analyzer equipped with an Ionspray ion source was scanned using the quadrapole, from a mass to charge (m/z) of 400–2000 units with a step size of 0.1 m/z and a 0.5-ms dwell time per step. The ion spray voltage and orafice potential were set at 4600 and 150 V, respectively.

Disulfide Bond Analysis. The number of disulfide bonds in mambin were quantitated according to the method of Thannhauser et al. (1984).

Circular Dichroism Spectra. Lyophilized mambin, kistrin, and erabutoxin *b* were each resuspended in 10 mM Tris-HCl, pH 7.5, to a concentration of ca. 1.0 mg/mL; exact protein concentrations were determined by quantitative amino acid analysis. Circular dichroism spectra were obtained on an Aviv Cary 60 spectropolarimeter, thermostated at 20 °C. All spectra are the average of five scans with an integration time of 2 s for each datum. Far-UV/CD spectra (190–250 nm) were obtained at an interval of 0.2 nm in a 0.01-cm cell.

Fg/GP IIb–IIIa ELISA and Platelet Aggregation Assays. The solid-phase Fg/GP IIb–IIIa ELISA and platelet aggregation assays were carried out as previously described (Dennis et al., 1990). A four-parameter fit (Marquardt, 1963) was used to estimate the half-maximal inhibition concentration (IC_{50}). IC_{50} values are reported as the average of two separate determinations.

Nicotinic Acetylcholine Receptor Binding Assays. Competition binding assays were carried out using a modified DEAE filter binding assay (Fong & McNamee, 1986). nAChR-containing membranes at a final concentration of 0.44 nM binding site were mixed with ^{125}I-α-Btx at 1.75 nM and sample and incubated for 90 min at 25 °C prior to spotting onto prewetted DEAE filter disks; nonspecific binding was measured in the presence of 3 μM cold α-Btx.

Sequence Alignment. The degree of overall sequence similarity of the short-chain neurotoxins was determined by calculating the average percentage of similar residues among all pairwise comparisons of the 32 aligned neurotoxin sequences presented by Dufton and Hider (1983). The average percentage of similar residues shared by mambin with the short-chain neurotoxins was similarly calculated. In assessing the similarity of two residues, the following conservative substitutions were allowed: Ile, Leu, Val, Met; Asp, Glu; Arg, Lys, His; Phe, Trp, Tyr; Thr, Ser; Gln, Asn. Ala, Gly, Pro, and Cys were considered unique.

On a per-residue basis, the degree of dissimilarity between mambin and the neurotoxins was scaled by the inherent degree of variability among the neurotoxins themselves to identify regions in which mambin was significantly distinct from the neurotoxins. To illustrate these regions of dissimilarity, the sequence of mambin was manually aligned with the sequences of erabutoxin *b* from *Laticauda semifasciata* (Smith et al., 1988) and representative short-chain neurotoxins from *Hemachatus haemachatus* (Strydom & Botes, 1971), *Dendroaspis viridis* (Banks et al., 1974), and *Dendroaspis polylepsis polylepsis* (Strydom, 1972).

Force-Field Calculations. All energy calculations were performed using the all-atom AMBER (Weiner et al., 1984, 1986) force field as implemented in version 2.6 of the Discover program (Biosym Technologies Inc., San Diego). A cutoff of 11.5 Å was used for nonbonded interactions; nonbonded interactions between 11.5 and 13.0 Å were attenuated using fifth-order polynomial switching functions. A linear dielectric ($\epsilon = 4.0$) was used to compensate for the lack of explicit solvent. All calculations were performed on a Silicon Graphics 4D/240 computer.

Model Construction. A model of mambin was constructed on the basis of the crystal structure of erabutoxin *b* (Smith et al., 1988) using the sequence alignment previously described. Most of the residues of mambin were generated by replacing the corresponding residues from erabutoxin *b* while retaining appropriate side-chain conformations. When required, loop conformations from other protein structures in the Brookhaven database (Bernstein et al., 1977) were used for amino acid sequences incompatible with the conformations found in erabutoxin *b*. Loop searching was performed by locating loops of appropriate length and composition that provided the best alignment of the backbone atoms of the residues preceding and following the region to be replaced. The model was assembled using version 2.5 of the Insight program (Biosym Technologies Inc., San Diego) running on a Silicon Graphics IRIS 4D/20 workstation; residue numbering is based on the erabutoxin *b* numbering system (see Figure 5).

The conformation of loop 1, extending from Arg-1 to Cys-17, was retained from the crystal structure of erabutoxin *b*; the conformation of Gln-20 to Asp-22 was derived from Ala-58 to Asn-60 of thermolysin [3TLN (Holmes & Matthews, 1982)] and required no significant perturbation of either Cys-17 or Ser-23.

Loop 2 of erabutoxin *b*, spanning residues Tyr-25 to Gly-40, is primarily β-sheet in nature. The major sequence differences in this loop between mambin and erabutoxin *b* occur between positions 30 and 35, during which the chain of erabutoxin *b* reverses direction via a type III β-turn initiated at Asp-31. In

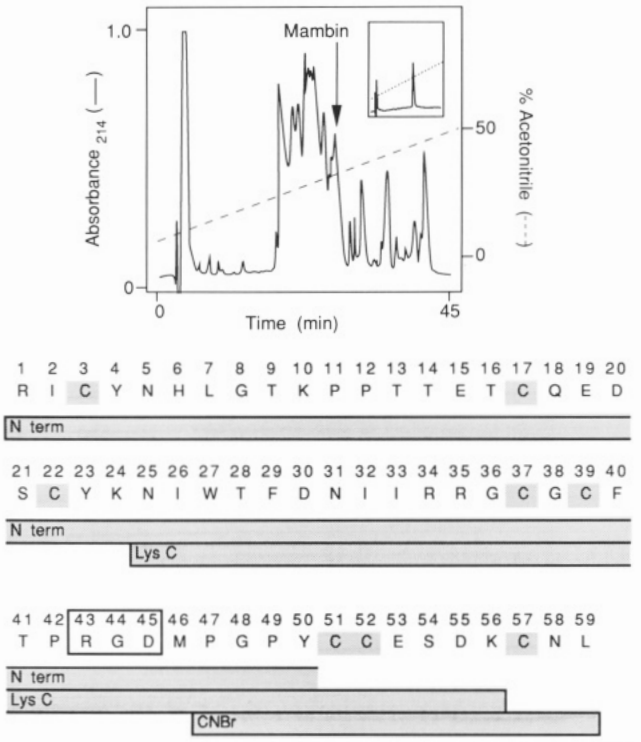

FIGURE 1: (a, top) Reverse-phase HPLC purification of mambin. Mambin (≈100 μg) was purified to homogeneity from 5 mg of *D. jamesonii* venom as described under Materials and Methods; active fractions were further purified by rechromatography (inset). (b, bottom) Amino acid sequence analysis of native mambin and the Lys-C and CNBr fragments used to align the sequence. Native protein and the Lys-C peptides were sequenced by Edman degradation; the shaded bars indicate the length of the sequence obtained and are in agreement with the total mass determined by electrospray ionization mass spectroscopy.

mambin, the conformation of Thr-32 through Asn-35 that accomplishes the chain reversal was taken a similar turn in the heavy chain of an immunoglobulin Fab [2FB4 (Kratzin et al., 1989), residues Lys-206 to Asn-209].

By far the most significant sequence difference between mambin and erabutoxin *b* occur in loop 3, between residues 44 and 54. In erabutoxin *b*, residues 51–53 adopt a β-strand conformation that forms an antiparallel set of hydrogen bonds with residues 28–26, respectively. Such a conformation is not feasible for the Pro-Gly-Pro sequence in positions 51–53 of mambin, suggesting that loop 3 of mambin may likely adopt a very different conformation than the corresponding loop in erabutoxin. A potential conformation of residues 44–54 that satisfied the constraints imposed by the presence of three prolines was generated; this conformation represents but one low-energy possibility.

The resulting model of mambin was energy-refined in four stages: first, the α-carbons of the portions of the model derived from erabutoxin *b* (residues 1–17, 24–28, 36–43, and 54–61) were held rigid, and the remainder of the molecule was minimized. In the second stage, a global minimization was performed until the maximum gradient was less than 0.01 kcal/Å. The resulting structure was refined using 10 ps of molecular dynamics at 300 K, followed by conjugate-gradient energy minimization to a maximum gradient of 0.001 kcal/Å.

Results

Purification of Mambin. Mambin was purified to apparent homogeneity from the venom of *D. jamesonii* by C18 reverse-phase HPLC (Figure 1a, inset). Samples from the HPLC profile were screened for GP IIb–IIIa antagonist activity using the solid-phase Fg/GP IIb–IIIa ELISA which

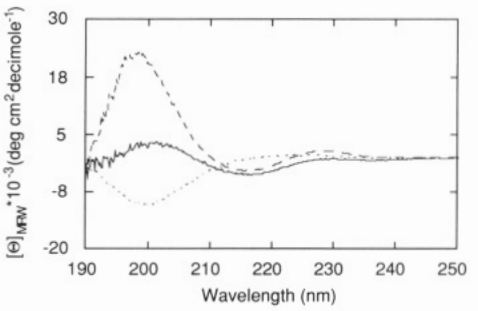

FIGURE 2: Circular dichroism spectrum of mambin. The circular dichroism spectroscopies of erabutoxin *b* (– –), mambin (—), and kistrin (···) were carried out as described under Materials and Methods.

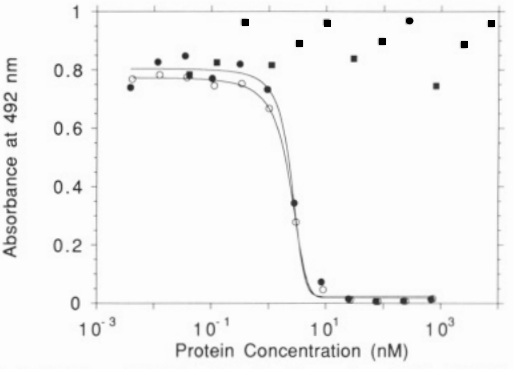

FIGURE 3: Inhibition of GP IIb–IIIa binding to immobilized fibrinogen by mambin, kistrin, and erabutoxin *b*. Inhibition of Fg/GP IIb–IIIa binding by mambin (○), kistrin (●), and erabutoxin *b* (■) was measured by a solid-phase ELISA assay (Dennis et al., 1990). Samples were diluted and added to the Fg-coated microtiter wells immediately preceding the addition of GP IIb–IIIa. Protein concentrations of the undiluted samples were determined by amino acid analysis. The IC_{50} values for mambin and kistrin were 3.1 ± 0.8 and 2.8 ± 0.8 nM, respectively; no inhibition was observed for erabutoxin *b* at concentrations <8 μM.

measures the inhibition of the binding of purified human platelet GP IIb–IIIa to immobilized Fg. A single active fraction was detected eluting at ca. 35% acetonitrile and was rechromatographed on HPLC (C18) to homogeneity (Figure 1a, inset). The yield of purified mambin from crude venom was ca. 2% (w/w). The activity of purified mambin was subsequently characterized by measuring in vitro inhibition of platelet aggregation as described below.

Protein Characterization and Spectral Analysis of Mambin. The amino acid sequence of mambin was determined by Edman degradation of the native protein and from peptides derived by CNBr hydrolysis and Lys-C proteolytic digestion and purified by reverse-phase HPLC; the amino acid composition agreed closely with that predicted from the protein sequence (data not shown). The peptide fragments used to determine the sequence of mambin are shown in Figure 1b. Mambin has 3.6 ± 0.3 disulfides determined experimentally, suggesting that all 8 cysteines are oxidized.

Electrospray ionization mass spectroscopy of the native molecule was used to corroborate the sequence analysis and verify that the complete sequence had been obtained. The observed molecular mass of 6744.2 ± 1.7 is in excellent agreement with the calculated molecular mass of 6745.66 for the native protein, allowing for the presence of four disulfide bonds. The circular dichroism spectra of mambin, erabutoxin *b*, and kistrin at pH 7.5 are shown in Figure 2. The CD bands at 195 and 215 nm for mambin and erabutoxin *b* are consistent with significant β-sheet content observed for the neurotoxins (Dufton & Hider, 1983); the kistrin spectrum does not indicate any secondary structure.

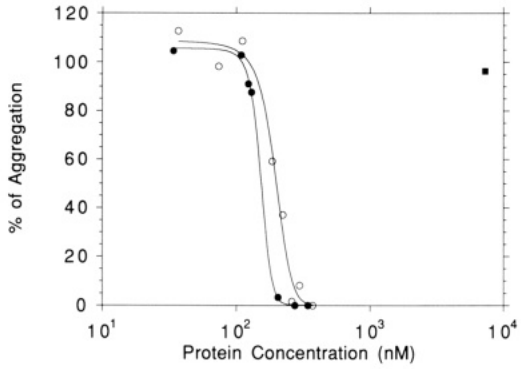

FIGURE 4: Inhibition of platelet aggregation by mambin, kistrin, and erabutoxin *b*. Inhibition of ADP-induced platelet aggregation in human platelet rich plasma by mambin (○), kistrin (●), and erabutoxin b (■) was measured as previously described (Dennis et al., 1990). The IC_{50} values for mambin and kistrin were 172 ± 22 and 113 ± 21 nM, respectively; no inhibition was observed for erabutoxin *b* at 8 μM.

Antagonism of GP IIb–IIIa and Inhibition of Human Platelet Aggregation. The determination of the specific activity (IC_{50}) of mambin was measured by its ability to inhibit the binding of purified human platelet GP IIb–IIIa to immobilized Fg (IC_{50} = 3.1 ± 0.8 nM) using the Fg/GP IIb–IIIa, ELISA (Figure 3); reduced and carboxymethylated mambin was inactive. The peptide cyclo-C43–C54 exhibited an IC_{50} value of 5.0 nM in the Fg/GP IIb–IIIa ELISA. Mambin inhibited platelet aggregation in ADP-stimulated human platelet rich plasma (PRP) in a dose-dependent manner with an IC_{50} value of 172 ± 22 nM (Figure 4). No activity was observed for erabutoxin *b* in either of the above assays at 8 μM, the highest concentration tested (Figures 3 and 4). Kistrin, a GP IIb–IIIa antagonist and platelet aggregation inhibitor from the *Viperidae* family (Dennis et al., 1990), exhibited IC_{50} values of 2.8 ± 0.8 and 113 ± 21 nM in the Fg/GP IIb–IIIa ELISA (Figure 3) and platelet aggregation assays (Figure 4), respectively.

Antagonism of Nicotinic Receptor Binding. Since the mambin sequence is very similar to the short- and long-chain neurotoxin sequences (see below), competition binding was carried out between ^{125}I-α-bungarotoxin, a well-characterized long-chain neurotoxin from *Bungarus multicinctus* (Love & Stroud, 1986), and nicotinic acetylcholine receptor (nAChR) from *T. californica*. Erabutoxin *b* exhibited a K_D value of ca. 200 pM comparable to that previously reported (Ishikawa et al., 1977) and completely inhibited binding at 25 nM; however, no inhibition of binding was detected by mambin at a concentration of 100 μM (n = 3; data not shown).

Sequence Alignment. The 32 short-chain neurotoxins presented by Dufton and Hider (1983) share an overall sequence identity of 70.4% with a sequence similarity of 74.8%. Mambin shares 40.6% identity and 47.1% similarity to these short-chain neurotoxins as a group; it is slightly more similar to erabutoxin *b* (46.0% sequence identity and 55.6% similarity). Mambin contains 16 of the 25 invariant residues found in the short-chain neurotoxins, including all 8 cysteines. These 16 residues are generally located near the core of the molecule, based on the erabutoxin *b* crystal structure. The sequence alignment of mambin with representative GP IIb–IIIa protein antagonists from *Viperidae* venoms (boxed) and representative short-chain neurotoxins from *Elapidae* venoms (shaded) is shown in Figure 5. Also shown are the invariant residues from the neurotoxins.

Model Construction. Superimposition of the α-carbon coordinates of residues 1–17, 24–29, 36–43, and 54–62 of the energy-refined mambin model with the corresponding residues from the erabutoxin *b* crystal structure gave an rms deviation of 0.6 Å, suggesting that the loop replacements induced little perturbation of the core structure. The resulting superimposed α-carbon coordinates and the invariant residues present in all

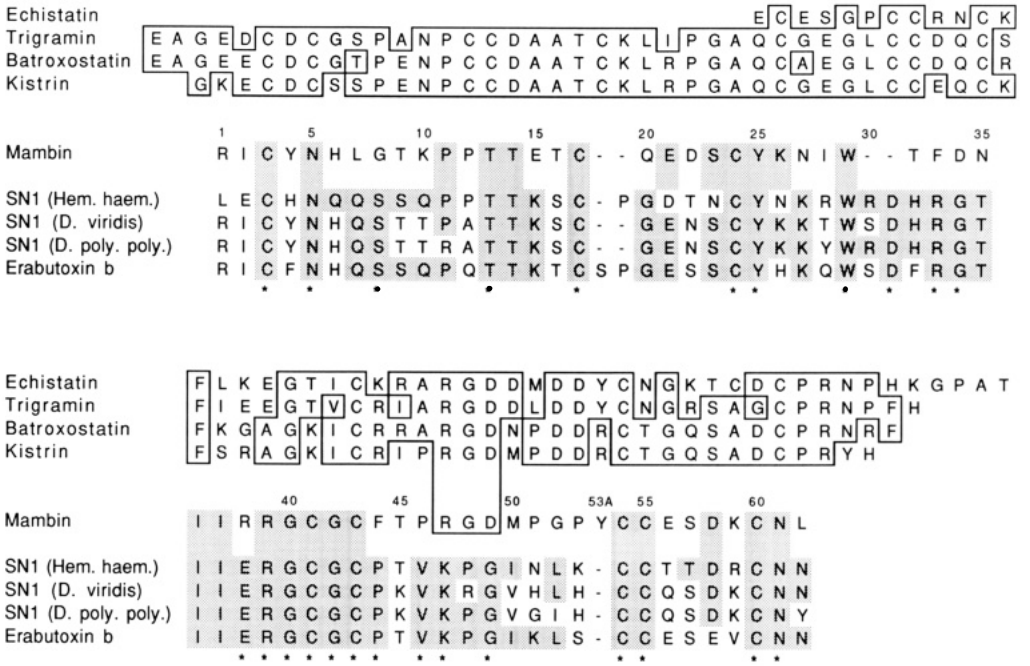

FIGURE 5: Sequence comparison of *Viperidae* snake venom GP IIb–IIIa antagonists, mambin, and *Elapidae* snake venom short-chain neurotoxins. Sequences are shown for echistatin from *Echis carinatus* (Gan et al., 1988), trigramin from *Trimeresurus gramineus* (Huang et al., 1989), batroxostatin from *Bothrops atrox* (Rucinski et al., 1990), kistrin from *A. rhodostoma* (Dennis et al., 1990), mambin, short neurotoxin 1 from *H. haemachatus* (Strydom & Botes, 1971), short neurotoxin 1 from *D. viridis* (Banks et al., 1974), short neurotoxin 1 from *D. polylepsis polylepsis* (Strydom, 1972), and erabutoxin *b* from *L. semifasciata* (Smith et al., 1988); the numbering scheme used in discussions of the mambin sequence is shown. Residues which are identical in at least 50% of the sequence of the *Viperidae* GP IIb–IIIa antagonists are boxed; residues which are identical in at least 50% of the 32 sequences of the short-chain neurotoxins (Dufton and Hider, 1983) are shaded; residues that are invariant in the short-chain neurotoxins are noted below with an asterisk. The RGD sequence common to each of the platelet aggregation inhibitors is also boxed.

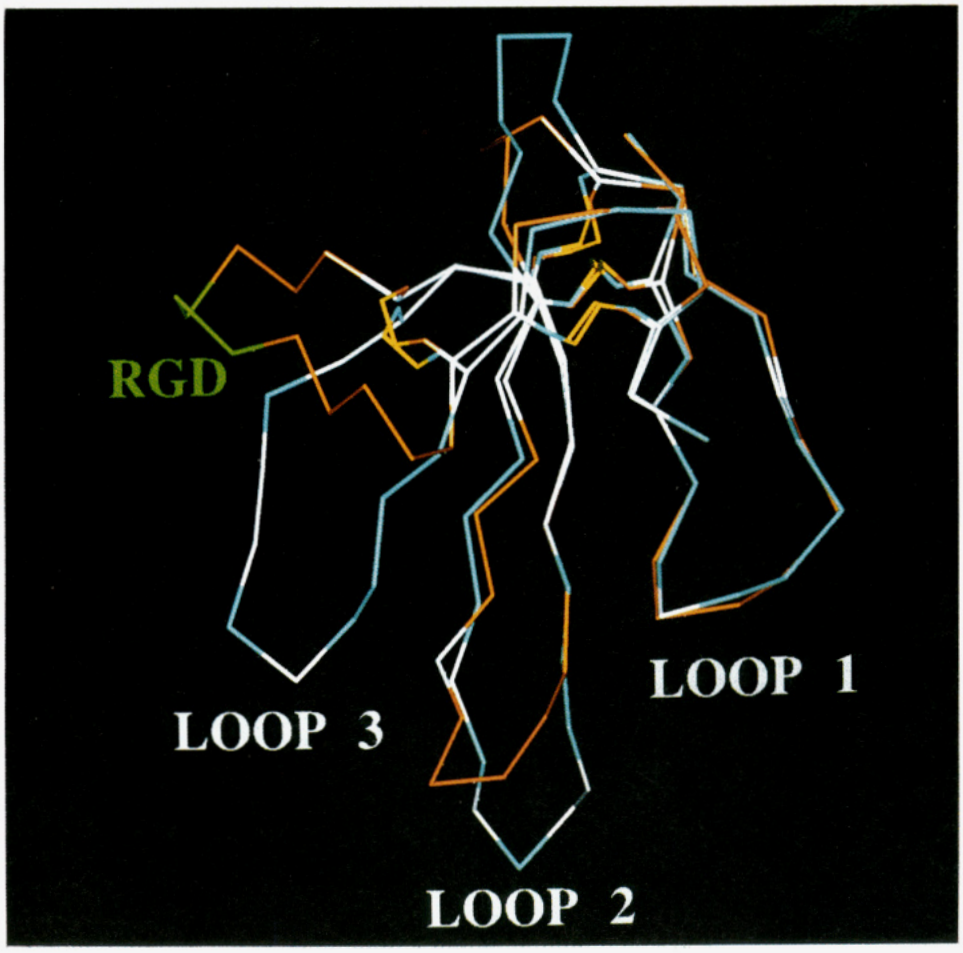

FIGURE 6: Superimposed α-carbon coordinates for erabutoxin *b* and the proposed model of mambin. Mambin is shown in brown and erabutoxin *b* in light blue. Invariant residues of the short-chain neurotoxins are shown in white. Also shown are the cysteine side chains of both molecules in yellow. The RGD sequence of mambin is indicated in green.

short-chain neurotoxins are shown in Figure 6. Of the invariant residues present in mambin, all are found in similar positions in the predicted model. The overall structure predicted for mambin was stable during the dynamics phase of the refinement: the α-carbons of structures minimized before and after dynamics had an rms deviation of 1.0 Å.

Discussion

Mambin has been purified from the venom of the *Elapidae* snake *D. jamesonii* and characterized as a potent platelet aggregation inhibitor and GP IIb–IIIa antagonist. The primary sequence of mambin is 59 residues long and contains four disulfide linkages as well as the RGD adhesion site recognition sequence, common to many adhesion proteins (Phillips et al., 1988; Plow & Ginsburg, 1989; Ruoslahti & Pierschbacher, 1987). Although comparable in cysteine content (14%) and equipotent in activity as a GP IIb–IIIa antagonist and platelet aggregation inhibitor, mambin bears little sequence similarity (Figure 5) to any of the proteins from the *Viperidae* venom inhibitor family (Dennis et al., 1990; Gould et al., 1990) or the leech GP IIb–IIIa antagonists decorsin (Seymour et al., 1990) or ornatin (Mazur et al., 1991). The only similarity between mambin and these proteins lies within the RGD region (Figure 5, boxed region). Like other disulfide-rich GP IIb–IIIa protein antagonists (Huang et al., 1987; Gan et al., 1988; Dennis et al., 1990), the tertiary structure of mambin is critical for potent activity.

The most enlightening data for mambin come from a comparison of its sequence with those in the NBRF-PIR database (George et al., 1986), which reveals a striking similarity to sequences of the short-chain neurotoxins (Figure 5, shaded region). In fact, a protein named S5C1 that differs by only six residues from mambin has been described but was not characterized other than failing to exert a toxic effect on mice at a dose of 130 μg/g body weight (Joubert & Taljaard, 1979); LD_{50} values for typical short-chain neurotoxins such as erabutoxin *b* are ca. 0.1 μg/g body weight (Tamiya & Arai, 1966). Excluding the RGD region, mambin shares considerable sequence similarity with erabutoxin *b*, including the conserved cysteine residues that form the core of both short- and long-chain neurotoxins (Dufton & Hider, 1983). In the neurotoxins, this core connects the termini of three major loops that are largely β-sheet in nature. The β-sheet content of loops 1 and 2 of mambin is predicted to be similar to that of erabutoxin *b* (Figure 6). In loop 3 of erabutoxin *b*, the β-sheet content is localized in residues 51–53; the Pro-Gly-Pro sequence in the corresponding region of mambin is incompatible with a β-sheet conformation. On the basis of these arguments, mambin is predicted to display a reduced degree of β-sheet structure relative to erabutoxin *b*, as reflected in the circular dichroism spectra (Figure 2).

In the proposed model of mambin, the RGD sequence is located on the apex of a loop that points away from the bulk of the protein. The model suggests, on the basis of the conserved disulfide positions found in the short-chain neurotoxins (Dufton & Hider, 1983; Low & Corfield, 1988), that this loop is formed by a disulfide bond between cysteines 43 and 54; the cyclic peptide cyclo-C43–C54 derived from this loop likewise displays a potency in the Fg/GP IIb–IIIa ELISA comparable to that of mambin itself. In the 2D NMR-derived

structures of kistrin (Adler et al., 1991) and echistatin (Cooke et al., 1991; Dalvit et al., 1991; Saudek et al., 1991), the RGD sequence is also at the apex of a hairpin loop. The detailed conformations of the RGD sequences in both the kistrin and echistatin loops are ill-defined due to sparse long-range NOE signals, thereby preventing a quantitative comparison with the proposed conformation in the mambin model. It is noteworthy that proteins of very different overall structures are able to present the RGD adhesion site recognition sequence in an apparently similar orientation at the tip of a hairpin loop.

Mambin, in addition to bearing little sequence similarity to the *Viperidae* venoms kistrin and echistatin, is also topographically distinct from these proteins, whose NMR structures have recently been reported (Adler et al., 1991; Cooke et al., 1991; Dalvit et al., 1991; Saudek et al., 1991). Although all three proteins consist largely of irregular loops connected via disulfide bridges, the disulfide patterns derived for kistrin (Adler et al., 1991) and echistatin (Saudek et al., 1991), which share a similar overall fold, are significantly different from the pattern proposed for mambin. The resulting loops created by those disulfides are likewise oriented quite differently in mambin than in the other two proteins. These structural differences make it unlikely that mambin is related to the RGD-containing *Viperidae* venoms, suggesting that the binding of these proteins to GP IIb–IIIa and their comparable potency as platelet aggregation inhibitors are solely determined by the appropriate presentation of the RGD sequence. This conclusion is further supported by the fact that small cyclic RGD-containing peptides inhibit platelet aggregation with potency similar to that of the proteins (Barker et al., 1991).

The structures and interactions of the short- and long-chain neurotoxins with the nicotinic acetylcholine receptor have been well studied (Low & Corfield, 1988; Stroud et al., 1990). Typical dissociation constants for the neurotoxins with the nAChR range from 10^{-10} to 10^{-11} M. The binding of neurotoxins to the nAChR involves a multicontact site defined by the concave surface of the β-sheet formed by the second and third loops of the protein (Dufton et al., 1989; Endo & Tamiya, 1987; Love & Stroud, 1986); this surface is largely hydrophobic in nature. Although the specific residues implicated in binding have not been determined, an analysis of conserved residues present in both short- and long-chain neurotoxins coupled with the results of chemical modifications of side chains has implicated the following residues as contributing significantly to receptor binding (erabutoxin *b* numbering scheme): Lys-27, Trp-29, Asp-31, Phe(His)-32, Arg-33, and Lys-47 (Dufton & Hider, 1983). These residues occur in the second and third loops, where mambin is least similar to the short-chain neurotoxins; the absence of most of these residues almost certainly accounts for the lack of binding between mambin and the nACh receptor. Erabutoxin *b* did not display any GP IIb–IIIa antagonist or platelet aggregation inhibitory activity, presumably due to the lack of an RGD sequence.

The finding that an *Elapidae* snake has a protein with the general structure of a neurotoxin, but with the function of a platelet aggregation inhibitor, is unique and may have important implications for evolutionary biology. Snakes belonging to the family *Viperidae* have been thought to affect their prey primarily through hemotoxic proteins, whereas those belonging to family *Elapidae* are well-known for acting primarily via neurotoxic proteins. The short-chain neurotoxins found in *Elapidae* snake venoms have been proposed to have diverged from an ancestral phospholipase–RNase-like protein (Strydom, 1979); the evolution of toxins from *Viperidae* venoms has not been well studied. The venoms of the *Dendroaspis* genus and *D. jamesonii* in particular are known to contain short-chain neurotoxins (Joubert & Taljaard, 1979; Banks et al., 1974; Strydom, 1972). *Dendroaspis* venoms also contain a number of short-chain neurotoxin homologues which lack significant neurotoxicity due to the absence of key residues, yet retain the dominant structural features (including conserved cysteine residues) that define the fold of the short-chain neurotoxins (Dufton & Hider, 1983). It seems quite likely that mambin, which is an example of such a homologue, represents an evolutionary extension of these neurotoxins. Mambin may therefore represent a genetic hybrid of the neurotoxic nicotinic acetylcholine receptor antagonists and the hemotoxic GP IIb–IIIa antagonists found in snake venoms. This may occur either through a divergent pathway by gene duplication or by convergent evolution of unrelated proteins by exon shuffling (Doolittle, 1989; Gilbert, 1985). Mambin thus provides new insight into the role of structural protein chemistry and evolutionary biology for these classes of toxins. In addition to furthering our understanding of integin receptors, in particular, GP IIb–IIIa and its role in platelet aggregation, mambin, related proteins, and molecules with related structures have therapeutic potential for the treatment of thrombotic disease.

Acknowledgments

We thank Daryl Winter for his insight and interest, Jim Bourell for electrospray ionization mass spectra data, Suzy Wong for amino acid composition data, Craig Muir for providing purified Fg and ELISA assay data, Cliff Quan for peptide synthesis, Sherron Bullens for platelet aggregation data, and Tony Kossiakoff and Bob Stroud (UCSF) for their helpful discussions and support.

References

Adler, M., Lazarus, R. A., Dennis, M. S., & Wagner, G. (1991) *Science 253*, 445–448.

Albelda, S. M., & Buck, C. A. (1990) *FASEB J. 4*, 2868–2880.

Banks, B. E. C., Miledi, R., & Shipolini, R. A. (1974) *Eur. J. Biochem. 45*, 457–468.

Barany, G., & Merrifield, R. B. (1980) in *The Peptides* (Gross, E., & Meienhofer, J., Eds.) pp 1–284, Academic Press, New York.

Barker, P. L., Burnier, J. P., Gadek, T., & Thorsett, E. D. (1991) PCT Intl. Appl. WO 91 01331 (Feb 7, 1991).

Becker, R. C., & Gore, J. M. (1991) *Circulation 83*, 1038–1047.

Bernstein, F. C., Koetzle, T. F., Williams, G. J. B., Meyer, E. F., Brice, M. D., Rodgers, J. R., Kennard, O., Shimanouchi, T., & Tasumi, M. (1977) *J. Mol. Biol. 112*, 535–542.

Changeux, J. P., Devilliers-Thiery, A., & Chemoulli, P. (1984) *Science 225*, 1335–1345.

Coller, B. S., Folts, J. D., Scudder, L. E., & Smith, S. R. (1986) *Blood 68*, 783–786.

Cooke, R. M., Carter, B. G., Martin, D. M. A., Murray-Rust, P., & Weir, M. P. (1991) *Eur. J. Biochem. 202*, 323–328.

Dalvit, C., Widmer, H., Bovermann, G., Breckenridge, R., & Metternich, R. (1991) *Eur. J. Biochem. 202*, 315–321.

Dennis, M. S., Henzel, W. J., Pitti, R. M., Lipari, M. T., Napier, M. A., Deisher, T. A., Bunting, S., & Lazarus, R. A. (1990) *Proc. Natl. Acad. Sci. U.S.A. 87*, 2471–2475.

Doolittle, R. F. (1989) *Trends Biochem. Sci. 14*, 244–245.

Dufton, M. J., & Hider, R. C. (1983) *CRC Crit. Rev. Biochem. 14*, 113–171.

Dufton, M. J., Bladon, P., & Harvey, A. L. (1989) *J. Mol. Evol. 29*, 355–366.
Endo, T., & Tamiya, N. (1987) *Pharmacol. Ther. 34*, 403–454.
Fong, T. M., & McNamee, M. G. (1986) *Biochemistry 25*, 830–840.
Gan, Z.-R., Gould, R. J., Jacobs, J. W., Friedman, P. A., & Polokoff, M. A. (1988) *J. Biol. Chem. 263*, 19827–19832.
Garsky, V. M., Lumma, P. K., Freidinger, R. M., Pitzenberger, S. M., Randall, W. C., Veber, D. F., Gould, R. J., & Friedman, P. A. (1989) *Proc. Natl. Acad. Sci. U.S.A. 86*, 4022–4026.
George, D. G., Barker, W. C., & Hunt, L. (1986) *Nucleic Acids Res. 14*, 11–15.
Gilbert, W. A. (1985) *Science 228*, 823–824.
Gold, H. K., Coller, B. S., Yasuda, T., Saito, T., Fallon, J. T., Guerrero, J. L., Leinbach, R. C., Ziskind, A. A., & Collen, D. (1988) *Circulation 77*, 670–677.
Gould, R. J., Polokoff, M. A., Friedman, P. A., Huang, T.-F., Holt, J. C., Cook, J. J., & Niewiarowski, S. (1990) *Proc. Soc. Exp. Biol. Med. 195*, 168–171.
Hawiger, J. (1990) *Atheroscler. Rev. 21*, 165–186.
Holmes, M. A., & Matthews, B. W. (1982) *J. Mol. Biol. 160*, 623–639.
Huang, T.-F., Holt, J. C., Lukasiewicz, H., & Niewiarowski, S. (1987) *J. Biol. Chem. 262*, 16157–16163.
Huang, T.-F., Holt, J. C., Kirby, E. P., & Niewiarowski, S. (1989) *Biochemistry 28*, 661–666.
Ishikawa, Y., Menez, A., Hori, H., Yoshida, H., & Tamiya, N. (1977) *Toxicon 15*, 471–488.
Joubert, F. J., & Taljaard, N. (1979) *Biochim. Biophys. Acta 579*, 228–233.
Kieffer, N., & Phillips, D. R. (1990) *Annu. Rev. Cell Biol. 6*, 329–357.
Kratzin, H. D., Palm, W., Stangel, M., Schmidt, W. E., Friedrich, J., & Hilschmann, N. (1989) *Biol. Chem. Hoppe-Seyler 370*, 263–272.
Lee, C. Y. (1979) *Snake Venoms. Handbook of Experimental Pharmacology*, Springer-Verlag, Berlin.
Love, R. A., & Stroud, R. M. (1986) *Protein Eng. 1*, 37–46.
Low, B. W., & Corfield, P. W. R. (1988) in *Neurotoxins in Neurochemistry* (Dolly, I., & Oliver, J., Eds.) pp 13–26, Ellis Horwood Limited, Chichester.
Marquardt, D. W. (1963) *J. Soc. Ind. Appl. Math. 11*, 431–441.
Mazur, P., Henzel, W. J., Seymour, J. L., & Lazarus, R. A. (1991) *Eur. J. Biochem., 202*, 1073–1082.
McCarthy, M. P., & Stroud, R. M. (1989) *Biochemistry 28*, 40–48.
Phillips, D. R., Charo, I. F., Parise, L. V., & Fitzgerald, L. A. (1988) *Blood 71*, 831–843.
Plow, E. F., & Ginsburg, M. H. (1989) *Prog. Hemostasis Thromb. 9*, 117–156.
Rucinski, B., Niewiarowski, S., Holt, J. C., Soszka, T., & Knudsen, K. A. (1990) *Biochim. Biophys. Acta 1054*, 257–262.
Ruoslahti, E., & Pierschbacher, M. D. (1987) *Science 238*, 491–497.
Saudek, V., Atkinson, R. A., & Pelton, J. T. (1991) *Biochemistry 30*, 7369–7372.
Seymour, J. L., Henzel, W. J., Nevins, B., Stults, J. T., & Lazarus, R. A. (1990) *J. Biol. Chem. 265*, 10143–10147.
Smith, J. L., Corfield, P. W. R., Hendrickson, W, A., & Low, B. W. (1988) *Acta Crystallogr. A44*, 357–358.
Stocker, K. F. (1990) *Medical Use of Snake Venom Proteins*, CRC Press, Boca Raton, FL.
Stroud, R. M., McCarthy, M. P., & Shuster, M. (1990) *Biochemistry 29*, 11009–11023.
Strydom, D. J. (1972) *J. Biol. Chem. 247*, 4029–4042.
Strydom, D. J. (1979) in *Snake Venoms. Handbook of Experimental Pharmacology* (Lee, C. Y., Ed.) pp 258–275, Springer-Verlag, Berlin.
Strydom, D. J., & Botes, D. P. (1971) *J. Biol. Chem. 247*, 1341–1349.
Tamiya, N., & Arai, H. (1966) *Biochem. J. 99*, 624–630.
Thannhauser, T. W., Konishi, Y., & Scheraga, H. A. (1984) *Anal. Biochem. 138*, 181–188.
Weiner, S. J., Kollman, P. A., Case, D. A., Singh, U. C., Ghio, C., Alagona, G., Profeta, S., Jr., & Weiner, P. (1984) *J. Am. Chem. Soc. 106*, 765–784.
Weiner, S. J., Kollman, P. A., Nguyen, D. T., & Case, D. A. (1986) *J. Comput. Chem. 7*, 230–252.
Yasuda, T., Gold, H. K., Leinbach, R. C., Yaoita, H., Fallon, J. T., Guerrero, L., Napier, M. A., Bunting, S., & Collen, D. (1991) *Circulation 83*, 1038–1047.